Global Journal of Pure and Applied Mathematics.
ISSN 0973-1768 Volume 9, Number 3 (2013), pp. 307-316

http://www.ripublication.com/gjpam.htm

A Fourth Order Discontinuous Galerkin Scheme for the Elastodynamic Equations

Serge MOTO MPONG*, Nathalie GLINSKY†, Ste´phane LANTERI ‡ and Sarah DELCOURTE §

**University of Yaounde´ 1, Cameroon, serge moto@yahoo.com*
†IFSTTAR/CETE Nice & INRIA Sophia Antipolis-Me´diterrane´e, France
‡INRIA-Sophia Antipolis-Me´diterrane´e
§University of Lyon 1, France

Abstract

We present in this paper a fourth order discontinuous Galerkin method for the elastodynamic equations in the time domain. Our approach combines a fourth order spatial interpolation, centered fluxes and a fourth order leapfrog scheme for the time integration. Numerical results for the propagation of a 2D eigenmode are presented for second and fourth-order leapfrog schemes. We also propose a numerical study of the stability and the convergence of the method proving the accuracy of the scheme for both regular and irregular meshes.

Key words: time domain elastodynamic's equations, discontinuous Galerkin methods, ex- plicit leap-frog time scheme, numerical convergence, unstructured meshes

1 Introduction

Computational seismology has become a very important discipline for the study of seismic wave propagation, as analytical solutions only exist in few simple cases like homogeneous do- mains or simple geometries. Various numerical methods have been developped to solve such problems. Among them, we can mention the finite difference method [14][10], the classical finite element method [9][11], the spectral and pseudospectral methods [8], and the finite vol- ume method [3]. We choose to use a high-order Discontinuous Galerkin (DG) method applied to triangular meshes. The DG method has been initially introduced by Reed and Hill for the solution of the neutron transport equation. Neglected during many years, it is now very popu- lar to

solve hyperbolic problems. In spite of its success in many domains of applications, this method has been rarely applied to seismic wave propagation problems [12]. Ka¨ser et al. ([7] and many references therein) proposed a DG finite element scheme based on upwind fluxes and the ADER approach in order to solve the elastodynamic system with the same high accuracy in space and time. Antonietti et al [2] compared the Mortar spectral element method and the DG spectral element method, both on non conforming rectangular meshes, with a second or- der leapfrog scheme for the time integration. They found that those two methods have a good accuracy while used for the simulation of the elastodynamic equations. Agut et al [1] devel- opped a new high order method based on the "Modified Equation" technique in time, coupled with a DG method in space for the discretisation of the additional biharmonic operator, for the solution of the acoustic wave equation. Their results show that the computational cost of their scheme is the same as the one of the leapfrog scheme.

In this paper, we study the P-SV wave propagation in an isotropic, linear elastic medium by solving the velocity-stress formulation of the elastodynamic equations. Our method is based on centered fluxes and a leapfrog time-discretization which leads to a non dissipative scheme [4]. These are the differences between our approach and the one developped by Ka¨ser et al. [7]. According to the first results of the method presented in [4], the time accuracy of the scheme is crucial when global high-accuracy is required. Then, we propose an extension of the leapfrog scheme to a higher order of accuracy, following a method proposed for the Maxwell equations by Young [15] or Spachmann et al. [13] and applied to DG methods by Fahs [5]. This method allows us to achieve temporal accuracy to any even order desired by introducing an iterative procedure. We restrict here ourselves to the fourth-order leap-frog scheme since we consider a spatial interpolation based on fourth-degree polynomial functions at most. The method is applied to the propagation of an eigenmode in the unit square cavity. The numerical study of the stability and the convergence of the method is also studied for both regular and irregular meshes.

2 Equations and spatial discretization

In a linear, isotropic and infinite medium, the P-SV wave propagation is modelled by the elas- todynamic equation which can be written in velocity-stress formulation [14]

$$\begin{cases} \rho \partial_t \vec{v} &= \nabla \cdot \underline{\sigma} \\ \partial_t \underline{\sigma} &= \lambda (\nabla \cdot \vec{v}) \underline{I} + \mu (\nabla \vec{v} + (\nabla \vec{v})^t) \end{cases} \tag{1}$$

where ~v is the velocity vector, $\overline{\sigma}$ the stress tensor, ρ the density of the medium, $\underline{I}$ is the identity matrix and λ and μ the Lame´ coefficients describing the rheology of the medium, related to the P- and S-wave velocities by VP $=\sqrt{(\lambda + 2\mu)/\rho}$ and VS $=\sqrt{\mu/\rho}$. System (1) is closed by adding physical boundary conditions at the free surface of the medium : $\sigma \cdot \vec{n} = \vec{0}$, where $\vec{n}$ is the vector normal to the free surface. External forces are neglected.

Since the stress tensor is symmetrical, the unknown vector W may be written W~=(vx,vy,σxx,σyy,σxy)t and (1) expresses in matrix form as

$$\partial_t \vec{W} - \sum_{\alpha\in\{x,y\}} \underline{A}_\alpha(\rho,\lambda,\mu)\partial_\alpha \vec{W} = 0 \quad (2)$$

For the spatial discretization of this system, we approximate the physical domain by a polygon Ω, discretized in NT triangles Ti forming a partition of the domain. Each equation of (2) is multiplied by a scalar test function φTi and integrated on each element Ti. The characteristics of the medium (ρ, λ, μ) are assumed to be constant over each element Ti ; to simplify the notation, we denote by $A_\alpha^{T_i}$ in what follows, the restriction of the matrix $\underline{A}_\alpha(\rho,\lambda,\mu)\ to\ T_i$. Applying Green's identity, we obtain

$$\int_{T_i} \partial_t \vec{W}\varphi_k^{T_i} dxdy + \sum_{\alpha\in\{x,y\}} \underline{A}_\alpha^{T_i} \int_{T_{i_l}} \vec{W}\partial_\alpha \varphi_k^{T_i} dxdy - \underline{A}_n^{T_i} \int_{\partial T_i} \vec{W}\varphi_k^{T_i} ds = 0 \quad (3)$$

Where $\vec{n}$ is the outward unit normal vector to T_i and $\underline{A}_n^{T_i} = \sum_{\alpha\in\{x,y\}} n_\alpha \underline{A}_\alpha(\rho,\lambda,\mu)$.

As test function, we choose the standard Lagrange nodal interpolants φTi ∈ Pm(Ti), set of polynomials of degree m locally defined on the element Ti. Each component W of the vector $\vec{W}$ is approximated on Ti by

$$W_{|T_i}(x,y,z) = \sum_{j=1}^{N_m} W_j^{T_i}(t)\varphi_j^{T_i}(x,y),$$

where Nm is the number of basis functions and also the number of degrees of freedom on Ti. Including this approximation in (3), the first term writes

$$\forall k = 1,\cdots,N_m \ \int_{T_i} \partial_t \vec{W}\varphi_k^{T_i} dxdy = \sum_{j=1}^{N_m} \underline{M}_{kj}^{T_i} \frac{d}{dt}\vec{W}_j^{T_i} \ and\ \underline{M}_{kj}^{T_i} = \int_{T_i} \varphi_j^{T_i}\varphi_k^{T_i} dxdy\,,$$

where MTi is the mass matrix in the element Ti. Following the same method for the second integral of (3), we obtain

$$\forall k = 1,\cdots,N_m \ \sum_{\alpha\in\{x,y\}} \underline{A}_\alpha^{T_i} \int_{T_i} \vec{W}\partial_\alpha \varphi_k^{T_i} dxdy = \sum_{\alpha\in\{x,y\}}^{N_m} \underline{A}_\alpha^{T_i} \sum_{j=1}^{N_m} \underline{G}_{\alpha,kj}^{T_i} \vec{W}_j^{T_i}$$

$$where\ \underline{G}_{\alpha,kj}^{T_i} = \int_{T_i} \varphi_j^{T_i}\partial_\alpha \varphi_k^{T_i} dxdy$$

For the last term of (3), the integral on ∂Ti, we split the boundary in internal and boundary faces. We define N (i) the set of the indices of the neighboring elements of Ti and Fil denotes each internal face common to the elements Ti and Tl (i.e. Fil = Ti ∩ Tl). Finally, B (i) is the set of the indices l of the faces which are common to Ti and the boundary of the domain ∂Ω. Such faces are denoted by F Bi = Ti ∩ ∂Ω for l ∈ B(i) ; The splitting of the boundary leads to

$$\underline{A}_n^{T_i} \int_{\partial T_i} \vec{W}\varphi_k^{T_i} ds = \sum_{l\in N(i)} \underline{A}_n^{T_i} \int_{F_{il}} \vec{W}\,\varphi_k^{T_i} ds + \sum_{l\in B(i)} \underline{A}_n^{T_i} \int_{F_l^{B_i}} \vec{W}\,\varphi_k^{T_i} ds \quad (4)$$

For an interior face, the associated boundary integral term is computed via the average value on this face $\vec{W}_{|F_{il}} = (\vec{W}^{T_i} + \vec{W}^{T_l})/2$. For a face $F_l^{B_i}$ on the boundary of the domain, the free surface condition $\underline{\sigma}\cdot\vec{n} = \vec{0}$ is introduced weakly in the second

term of (4). Finally, we define the vectors $\vec{V}_\alpha^{T_i}$ $(\alpha = x, y)$ and $\vec{S}_{\alpha\beta}^{T_i}$ $(\alpha, \beta = x, y)$ which contain respectively the N_m values of the velocity components vα and the three stress components σαβ in the element *Ti*. Thus, the spatial discretisation is summarized by

$$\begin{cases} \underline{M}^{T_i} \dfrac{d}{dt} \vec{V}_\alpha^{T_i} & = F_\alpha^{T_i}(\vec{S}) \quad \alpha = x, y \\ \underline{M}^{T_i} \dfrac{d}{dt} \vec{S}_{\alpha\beta}^{T_i} & = G_{\alpha\beta}^{T_i}(\vec{V}) \quad \alpha, \beta = x, y \end{cases} \tag{5}$$

where Fα and Gαβ are discrete operators collecting the integrals on Ti and ∂Ti.

3 Time discretization

For the time discretization, we apply an explicit leapfrog scheme which results, when combined with the flux, in a non-dissipative scheme [4]

$$\begin{cases} \underline{M}^{T_i} \dfrac{(\vec{V}_\alpha^{T_i})^{n+1} - (\vec{V}_\alpha^{T_i})^{n}}{\Delta t} & = F_\alpha^{T_i}(\vec{S}^{n+\frac{1}{2}}) \quad \alpha = x, y \\ \underline{M}^{T_i} \dfrac{(\vec{S}_{\alpha\beta}^{T_i})^{n+\frac{3}{2}} - (\vec{S}_{\alpha\beta}^{T_i})^{n+\frac{1}{2}}}{\Delta t} & = G_{\alpha\beta}^{T_i}(\vec{V}^{n+1}) \quad \alpha, \beta = x, y \end{cases} \tag{6}$$

where Δt is the time step of the scheme. Note that the initialisation of the scheme needs the velocities at t = t0 and the stresses at t = t0 + Δt/2. As this time discretization scheme is only second order accurate, the global accuracy of the scheme can be penalized when higher-degree polynomials (m > 2) are used for spatial approximation [4]. Then, we propose a higher-order leapfrog scheme following the method, proposed for the Maxwell's equations, by Young [15] or Spachmann et al. [13] and applied to a DG method by Fahs [5].

For a detailed description of the method, we introduce a simplified two equation problem whose unknowns are v(x, t) and σ(x, t)

$$\partial t v = f(\sigma) \text{ and } \partial t \sigma = g(v) \tag{7}$$

From Taylor developments, we can derive a leapfrog scheme based on velocities at even time steps and stresses at odd time steps. We rather choose to divide the time step by two and we obtain, for the simplified system (7)

$$\begin{cases} v^{n+1} = v^n + \Delta t \partial_t v^{n+\frac{1}{2}} + \dfrac{\Delta t^3}{24} \partial_{ttt} v^{n+\frac{1}{2}} + O(\Delta t^5) \\ \sigma^{n+\frac{3}{2}} = \sigma^{n+\frac{1}{2}} + \Delta t \partial_t \sigma^{n+1} + \dfrac{\Delta t^3}{24} \partial_{ttt} \sigma^{n+1} + O(\Delta t^5) \end{cases} \tag{8}$$

Firstly, the terms $\partial t\, v^{n+1/2}$ and $\partial t\, \sigma^{n+1}$ are evaluated using (7) at times (n+1/2) for V and (n + 1)Δt for σ. Considering only these derivatives in (8) and neglecting the higher-order terms leads to the classical second-order leapfrog scheme $v^{n+1} = v^n + \Delta t\, v_*^{n+\frac{1}{2}}$ and $\sigma^{n+\frac{3}{2}} = \sigma^{n+\frac{1}{2}} + \Delta t\, \sigma_*^{n+1}$ with $v_*^{n+1/2} = f(\sigma^{n+1/2})$ and $\sigma_*^{n+1} = g(v^{n+1})$. When applied to the discrete system (5), it is equivalent to the standard leap-frog scheme (6).

The construction of a higher order leapfrog scheme needs values for ∂ttt vn+1/2 and ∂ttt σn+1, obtained, as previously, by successive derivatives of (7). We then obtain a fourth-order leapfrog scheme

$$v^{n+1} = v^n + \Delta t\, v_*^{n+\frac{1}{2}} + \frac{\Delta t^3}{24} v_{**}^{n+\frac{1}{2}} \text{ and } \sigma^{n+\frac{3}{2}} = \sigma^{n+\frac{1}{2}} + \Delta t\, \sigma_*^{n+1} + \frac{\Delta t^3}{24}\, \sigma_{**}^{n+1} \tag{9}$$

$$\text{With } \begin{cases} \sigma_\circ^{n+\frac{1}{2}} = g\left(v_*^{n+\frac{1}{2}}\right) \\ v_{**}^{n+\frac{1}{2}} = f\left(\sigma_\circ^{n+\frac{1}{2}}\right) \end{cases} \text{ and } \begin{cases} v_\circ^{n+1} = f\left(\sigma_*^{n+1}\right) \\ \sigma_{**}^{n+1} = g\left(v_\circ^{n+1}\right) \end{cases}$$

This method is applied to (2) using the spatial discretization (5) and a fourth-order leapfrog scheme writes

$$\begin{cases} \left(\vec{V}_\alpha^{T_i}\right)^{n+1} = \left(\vec{V}_\alpha^{T_i}\right)^n + \Delta t \left(\vec{V}_\alpha^{T_i}\right)_*^{n+\frac{1}{2}} + \frac{\Delta t^3}{24}\left(\vec{V}_\alpha^{T_i}\right)_{**}^{n+\frac{1}{2}} & \alpha = x, y \\ \left(\vec{S}_{\alpha\beta}^{T_i}\right)^{n+\frac{3}{2}} = \left(\vec{S}_\alpha^{T_i}\right)^{n+\frac{1}{2}} + \Delta t \left(\vec{S}_{\alpha\beta}^{T_i}\right)_*^{n+1} + \frac{\Delta t^3}{24}\left(\vec{S}_{\alpha\beta}^{T_i}\right)_{**}^{n+1} & \alpha, \beta = x, y \end{cases} \tag{10}$$

With

$$\begin{cases} \left(\vec{V}_\alpha^{T_i}\right)_*^{n+\frac{1}{2}} = \left(\underline{M}^{T_i}\right)^{-1} F_\alpha^{T_i}\left(\vec{S}^{n+\frac{1}{2}}\right), \\ \left(\vec{S}_{\alpha\beta}^{T_i}\right)_\circ^{n+\frac{1}{2}} = \left(\underline{M}^{T_i}\right)^{-1} G_{\alpha\beta}^{T_i}\left(\vec{V}_*^{n+\frac{1}{2}}\right), \\ \left(\vec{V}_\alpha^{T_i}\right)_{**}^{n+\frac{1}{2}} = \left(\underline{M}^{T_i}\right)^{-1} F_\alpha^{T_i}\left(\vec{S}_\circ^{n+\frac{1}{2}}\right), \end{cases}$$

$$\begin{cases} \left(\vec{S}_{\alpha\beta}^{T_i}\right)_*^{n+1} = \left(\underline{M}^{T_i}\right)^{-1} G_{\alpha\beta}^{T_i}\left(\vec{V}^{n+1}\right) \\ \left(\vec{V}_\alpha^{T_i}\right)_\circ^{n+1} = \left(\underline{M}^{T_i}\right)^{-1} F_\alpha^{T_i}\left(\vec{S}_*^{n+1}\right) \\ \left(\vec{S}_{\alpha\beta}^{T_i}\right)_{**}^{n+1} = \left(\underline{M}^{T_i}\right)^{-1} G_{\alpha\beta}^{T_i}\left(\vec{V}_\circ^{n+1}\right) \end{cases}$$

In practice, for a given approximation in space, the fourth-order leapfrog scheme needs three times the number of arithmetic operations (to calculate the fluxes F and G) than the classical leapfrog scheme and twice as much memory storage since additional arrays have to be defined for $\left(\vec{V}_\alpha^{T_i}\right)_{**}^{n+\frac{1}{2}}$ and $\left(\vec{S}_{\alpha\beta}^{T_i}\right)_{**}^{n+1}$.

4 Numerical results

We realize some numerical studies of the properties of the method. A mathematical analysis of the stability and convergence of this new scheme is underway and will be the subject of a further publication. The method has been first applied to the propagation of an eigenmode. The computational domain D is the unit square and free surface boundary conditions are applied on all boundaries. We consider the (1,1)

mode whose exact solution is [6]

$v_x = a \cos \pi x \sin \pi y \cos at \quad \sigma_{xx} = -b \sin \pi x \sin \pi y \sin at$

$v_y = -a \sin \pi x \cos \pi y \cos at \quad \sigma_{yy} = b \sin \pi x \sin \pi y \sin at$

$\sigma_{xy} = 0$

where $a = \sqrt{2}\pi V_s \; and \; b = 2\pi.$ (11)

The medium properties are $\rho = 1$, $\lambda = 0.5$ and $\mu = 0.25$, leading to $Vp = 1$ and $VS = 0.5$.

The initialisation of the leapfrog scheme is done from the exact solution (11) at $t = 0$ for v and $t = \Delta t/2$ for σ, Δt being the time step of the scheme. The notation Pk-LFi (k=1,..., 4 and i=2 or 4) refers to a spatial discretization based on a polynomial basis of degree k and a classical second-order leapfrog time scheme (LF2) or its extension (LF4).

First, in order to check numerically the stability of the different methods, we solve this problem for different values of the time step. This time step depends on geometrical prop- erties of the mesh and is proportional to a CFL value which is a data of the simulation by $\Delta t = \text{MinTi h}[\text{C F L} \times hi/(Vp)_i]i$, a formula deduced from the optimal stability condition for finite volumes applied to the reference triangle (as in [4]) and where the mesh spacing hi is the smallest edge of the triangle Ti. We have performed such studies for all Pk-LFi combinations and the maximum values of the CFL numbers ensuring stability are given in the table 1. The value of the CFL number depends on both time and space schemes : its value decreases when the spatial discretization order increases and time steps of the LF4 schemes are greater than those of the LF2 schemes. For any space scheme, we have C F LLF4=2.5 × C F LLF2.

Table 1. Maximum CFL number for different methods

Time/space discretization	P2	P3	P4
LF2	0.2322	0.1498	0.0939
LF4	0.5928	0.3821	0.2644

For the convergence study of these schemes, we solve the problem using a series of meshes of different mesh spacing h. Uniform meshes are obtained by splitting quadrangular cells into two triangles and unstructured meshes are constructed via a mesher from an uniform distribution of the nodes on the boundaries of the domain. The mesh spacing h is the smallest edge in the mesh. All results correspond to solutions at time t = 5.0 s. We display, in figure 1, the L2- error between computed and exact solutions as a function of h for different schemes applied to regular (left figure) and irregular meshes (right figure) and using the classical leapfrog scheme (LF2, first line of figures). The convergence is second order for both types of meshes, even if the error level is lower for the highest order schemes. The use of higher degree basis function do not improve the convergence of the scheme. The results for

unstructured meshes are slightly better than those for uniform meshes. This is probably due to the choice of Delaunay meshes which have well known properties [4].

We present, in Figure 1, the same results for the fourth-order leapfrog extension (LF4, second line of figures), for uniform (left figure) and unstructured meshes (right figure). Con- vergence is clearly improved when high-order time schemes are used, for both types of meshes. In particular, for P3-LF4 and P4-LF4 methods, a fourth-order convergence is obtained. This proves that the use of fourth-degree basis functions (P4) is optimal when combined to a fourth- order time scheme (LF4). In summary, the values of the convergence orders of the different methods, are collected in Table 2 and confirm the results of the figures.

Table 2. Values of convergence orders of different methods

	Mesh	LF2	LF4		Mesh	LF2	LF4		Mesh	LF2	LF4
P2	Unif.	2.44	3.04	P3	Unif.	2.07	3.50	P4	Unif.	2.00	4.47
	Unstr.	2.57	2.92		Unstr.	2.42	3.03		Unst.	2.01	4.01

Finally, we examine the efficiency of the different methods by plotting, in Figure 2, for uni- form meshes, the evolution of the L2-error at time t = 5.0 s as a function of the CPU time of the simulation. For a given level of accuracy, the two most accurate methods (P3-LF4 and P4-LF4) are also the most efficient since the given error level is obtained for lower CPU times. The ratio between the minimum and the maximum CPU times to reach the given level of accuracy, corresponding respectively to the P4-LF4 and P2-LF2 schemes is about 100. The LF4 scheme needs more operations but higher-order schemes are more efficient as coarser meshes can be used to reach a desired accuracy level. The use of greater times steps in the LF4 scheme case compensates for the extra cost due to the multi-step procedure.

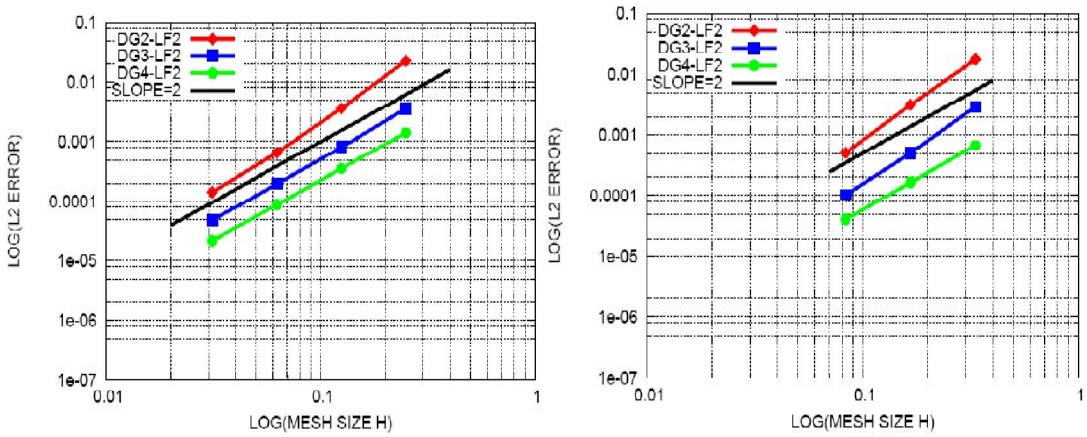

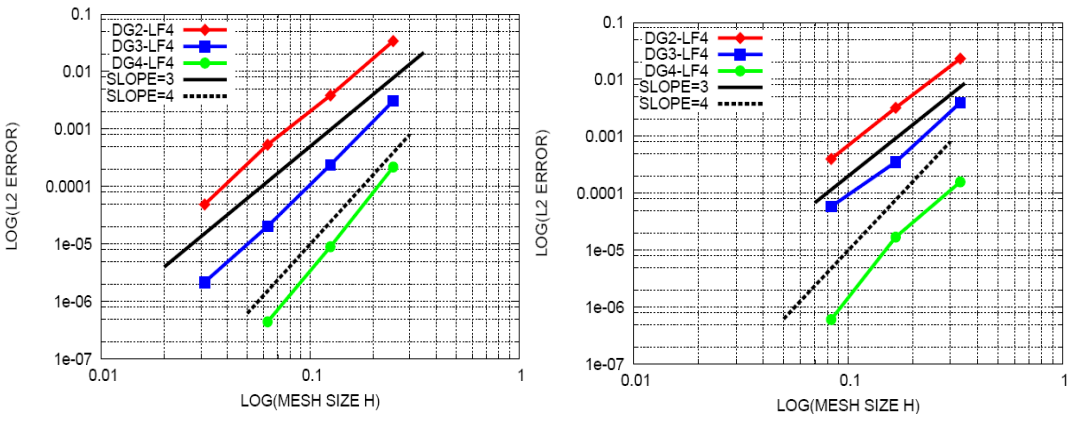

Figure 1: Convergence study. L2-error as a function of the mesh spacing h for Pk-LF2 schemes (k=2,3,4) (first line) and Pk-LF4 schemes (second line) using uniform (left) and unstructured meshes (right).

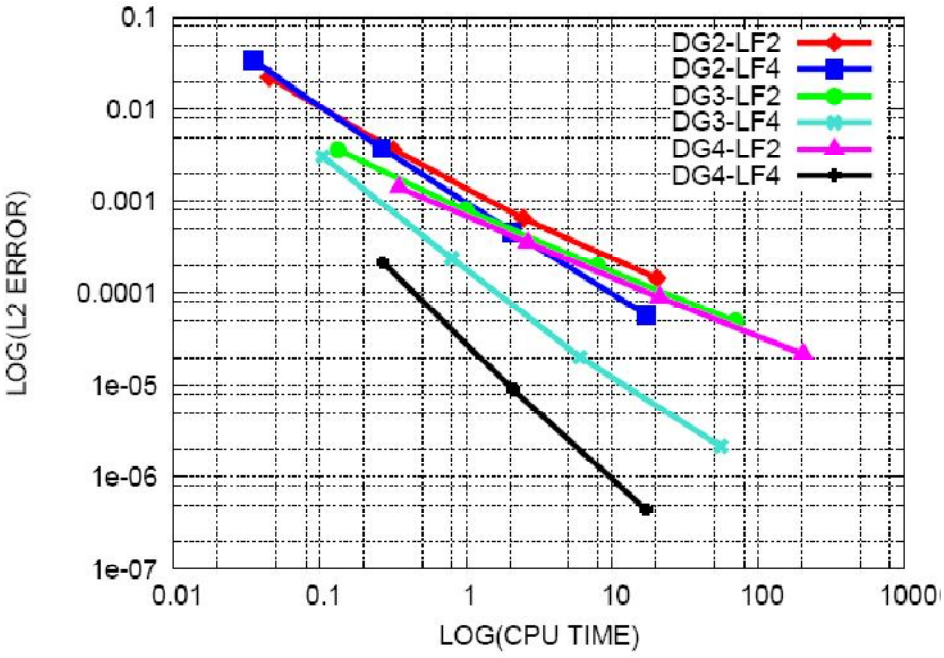

Figure 2: Efficiency of the methods. L2-error at time t = 5.0 s as a function of CPU time for Pk-LFi schemes (k=2,3,4, i=2 or 4) (uniform meshes).

5 Conclusion

We proposed a fourth-order leapfrog time scheme combined with a high-order discontinuous Galerkin method for the solution of the elastodynamic equations. Following the previous results obtained in [4], when global high-order accuracy is sought, it is worth to use higher- order space interpolation while keeping the classical leapfrog time scheme since accuracy is not improved while CPU costs are increased.

This extension of the leapfrog scheme to fourth-order modifies the classical leapfrog scheme in a multi-step procedure but where the additional cost is compensated by the use of greater time steps. This method has been applied to the propagation of an eigenmode which permits numerical studies of stability, convergence, accuracy and efficiency of the scheme. Note that fourth-order convergence is attained with the P4-LF4 version, when it is limited to second order when the classical leapfrog scheme is used.

References

[1] C. Agut, J. Diaz and Abdelaziz Ezziani, High-Order Schemes Combining the Modified Equation Approach and Discontinuous Galerkin Approximations for the Wave Equation, Commun. Comput. Phys., Vol. 11, No. 2, pp. 691-708 February 2012.

[2] P.F. Antonietti, I. Mazzieri, A. Quarteroni, F. Rapetti, Non-conforming high order approximations of the elastodynamics equation, Comput. Methods Appl. Mech. Engrg. 209-212 (2012) 212-238, 2012.

[3] M. Benjemaa, N. Glinsky-Olivier, V. M. Cruz-Atienza, J. Virieux and S. Piperno, Dynamic non-planar crack rupture by a finite volume method , Geophys. J. Int. 209-212 (2007) 212-238, 171, 271-285, 2007.

[4] S. Delcourte, L. Fezoui and N. Glinsky-Olivier, A high-order discontinuous Galerkin method for the seismic wave propagation, ESAIM : Proceedings, 27, 2009.

[5] H. Fahs, Méthode de type Galerkin discontinu d'ordre élevé pour la résolution numérique des équations de Maxwell instationnaires sur des maillages simplexes non-conformes, Thèse de doctorat de l'Université de Nice-Sophia Antipolis, 2008.

[6] N. Glinsky, S. Moto Mpong and S. Delcourte, A High-order Discontinuous Galerkin Scheme for Elastic Wave Propagation, Rapport de recherche INRIA, 7476, 2010.

M. Käser, V. Hermann and J. de La Puente, Accuracy alalysis of the Discontinuous Galerkin method for seismic wave propagation, Geophys. J. Int., 173, 3, 2008.

D. Komatitsch and J.-P. Vilotte, The spectral-element method: an efficient tool to simulate the seismic response of 2D and 3D geological structures , Bull. Seism. Soc. Am., 88, 368-392, 1998.

K. Marfurt, Accuracy of finite-difference and finite-element modeling of the scalar and elastic wave equations , Geophysics, 49 (5), 533-549, (1984).

P. Moczo, J. Kristek, V. Vavrycuk, R.J. Archuleta and L. Halada, 3D heterogeneous staggered-grid finite-difference modeling of seismic with volume harmonic and arithmetic averaging of elastic moduli and densities , Bull. Seism. Soc. Am., 92, 3042-3066, 2002.

[7] R. Mullen, T. Belytschko, Dispersion analysis of finite element semidiscretizations of the two-dimensional wave equation , Inter. J. Numer.

Meth. Engrg., 18 (1), 11-29, 1982.
W. Reed and T. Hill, Triangular mesh method for neutron transport equation, Tech. Rep. LA-UR-73-479, Los Alamos Scientific Laboratory, 1973.
H. Spachmann, R. Schuhmann, and T. Weilland, High order explicit time integration scheme for Maxwell-s equations, Int. J. Numer. Model., 15, 2002.
J. Virieux, P-SV wave propagation in heterogeneous media: Velocity-stress finite difference method, Geophysics, 51, 1986.
J. L. Young, High order leapfrog methodology for the temporally dependent Maxwell's equations, Radio Science, 36, 2001.